

An Approximate Wave-Number Domain Expression for Near-Field XL-MIMO Channel

Hongbo Xing, Yuxiang Zhang, Jianhua Zhang, Huixin Xu, Guangyi Liu and Qixing Wang

Abstract—As Extremely Large-Scale Multiple-Input-Multiple-Output (XL-MIMO) technology advances and carrier frequency rises, the near-field effects in communication are intensifying. A concise and accurate near-field XL-MIMO channel model serves as the cornerstone for investigating the near-field effects. However, existing wave-number domain XL-MIMO channel models under near-field conditions require non-closed-form oscillatory integrals for computation, making it difficult to analyze the channel characteristics in closed-form. To obtain a more succinct channel model, this paper introduces a closed-form approximate expression based on the principle of stationary phase. It was subsequently shown that when the scatterer distance is larger than the array aperture, the closed-form model can be further simplified as a trapezoidal spectrum. We validate the accuracy of the proposed approximation through simulations of power angular spectrum similarity. The results indicate that the proposed approximation can accurately approximate the near-field wave-number domain channel within the effective Rayleigh distance.

Index Terms—near-field, XL-MIMO, wave-number domain, the principle of stationary phase.

I. INTRODUCTION

EXTREMELY Large-Scale Multiple-Input-Multiple-Output (XL-MIMO) stands out as a pivotal technology within the sixth generation mobile communication systems (6G) [1]. By deploying extremely large antenna arrays in massive MIMO, it is hoped to achieve higher spectrum efficiency and higher energy efficiency [2]. An accurate and tractable channel model is essential for thorough exploration and utilization of XL-MIMO [3]. However, as the array aperture increases and the carrier frequency rises [4], the near-field region will expand [5], scatterers will be more likely to appear in the near-field region [6], [7]. At this point, the spherical wave assumption should be used to replace the plane wave assumption in channel modeling [8].

Most existing XL-MIMO near-field channel models are based on the parametric physical models [6]–[9], which model the channel as a sum of different multipaths in spatial or angular domains [10]. In spatial domain, the multipaths are modeled using array response vectors, where the array response vectors are obtained through spherical wave assumption. In angular domain, traditional MIMO angular domain

channel expression is based on the plane wave assumption, which utilizes the Fourier transform to map the multipath onto a set of angular domain orthogonal bases, thus creating a sparse, orthogonal channel expression [11]. However, since the plane wave assumption fails in near-field region, it is not possible to directly extend it to the near-field XL-MIMO.

Recently, a novel XL-MIMO channel model called the Fourier plane-wave series expansion has been presented [12]. By performing continuous Fourier transform in three dimensions, the electromagnetic wave is decomposed into a series of weighted sums of different oriented plane waves, thus the spatial domain channel is transformed into wave-number domain. In terms of definition, the wave-number domain is more general than the angular domain, as it is applicable in both near-field and far-field environments. Near-field channel model in wave-number domain enables near-field beam training [13] and near-field channel characteristics analysis [14]. However, due to the nonlinear characteristics of the spherical wave phase, computing the near-field wave-number domain channel requires non-closed-form oscillatory integral, making quantitative analysis challenging.

On this basis, it is hoped to investigate a closed-form wave-number domain channel expression. Inspired by the similarity between spherical wave and Frequency-modulated (FM) signal, we employ the Principle of Stationary Phase (POSP) [15] from the field of radar signal processing to derive the approximation of the near-field wave-number domain channel. Specifically, the precise non-closed-form integral expression for the wave-number domain channel is derived based on the existing near-field spatial domain channel model for XL-MIMO. Moreover, a closed-form approximation of the wave-number domain channel is derived based on POSP. This approximation disregards the oscillations present in the precise solution and describes the power spread range and power distribution in the wave-number domain. Furthermore, it is noted that the proposed approximation can be further simplified when the scatterer distance is larger than the array aperture. The simplified approximation takes the form of a trapezoidal function on a symmetric interval, which is both simpler and more tractable. Finally, the accuracy and applicability of the proposed approximation are evaluated based on the simulation results of the Power Angular Spectrum (PAS) similarity percentage [16].

II. EXISTING NEAR-FIELD XL-MIMO CHANNEL MODEL

In this section, we primarily discuss the existing near-field XL-MIMO channel models. As for spatial domain, we present

Hongbo Xing, Yuxiang Zhang, Jianhua Zhang and Huixin Xu are with the State Key Lab of Networking and Switching Technology, Beijing University of Posts and Telecommunications, Beijing 100876, China (e-mail: hbxing@bupt.edu.cn; zhangyx@bupt.edu.cn; jhzhang@bupt.edu.cn; xuhuixin@bupt.edu.cn).

Guangyi Liu and Qixing Wang are with the Future Research Laboratory, China Mobile Research Institute, Beijing 100053, China (e-mail: liuguangyi@chinamobile.com; wangqixing@chinamobile.com)

existing multipaths model based on array responses. As for wave-number domain, we discuss the wave-number domain expression and the relation between wave-number domain and angular domain. Without loss of generality, we discuss only two uniform linear arrays (ULA) placed in the same plane as receiver and transmitter, reducing the three-dimensional spatial channel to two dimensions. Note that it is possible to extend the present model into a three-dimensional model.

A. Spatial Domain Expression

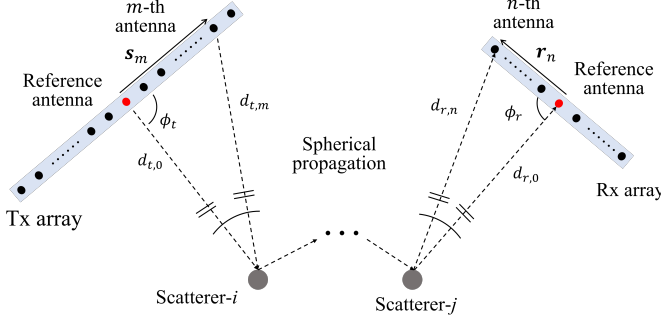


Fig. 1: When the scatterer is in the near-field region, $h(\mathbf{r}, \mathbf{s})$ needs to be calculated by using the spherical wave assumption

We consider an XL-MIMO channel with near-field multipaths, the transmitter and receiver are both ULA with array apertures D_t , D_r , respectively. As shown in Fig. 1. According to the Green's function method, the channel response h_{mn} between any two transceiver antenna pairs can be modeled as a function with the transceiver antenna coordinates \mathbf{r} , \mathbf{s} as independent variables [12], i.e., $h_{mn} = h(\mathbf{r}_m, \mathbf{s}_n)$. For the channel with single near-field path, h_{mn} can be modeled by the near-field array response vectors [7] and $h(\mathbf{r}, \mathbf{s})$ can be expressed as

$$h(\mathbf{r}, \mathbf{s}) = \alpha g(\mathbf{r}, \mathbf{d}_{r,0}) \cdot g^*(\mathbf{s}, \mathbf{d}_{t,0}), \quad (1)$$

where α is the complex amplitude of the path, $\mathbf{d}_{t,0}$ and $\mathbf{d}_{r,0}$ are the position vector from the reference antenna of Tx/Rx array to the first/last scatterer. Define $\mathbf{d}_{t,m}$ and $\mathbf{d}_{r,n}$ to be the position vector from a given antenna to the first/last scatterer, according to the geometric relation, there are $\mathbf{d}_{r,n} = \mathbf{d}_{r,0} - \mathbf{r}_n$ and $\mathbf{d}_{t,m} = \mathbf{d}_{t,0} - \mathbf{s}_m$. $g(\mathbf{r}, \mathbf{d}_{r,0})$ is the near-field array response function, describing the amplitude and phase of antenna at position \mathbf{r} relative to the reference antenna:

$$g(\mathbf{r}, \mathbf{d}_{r,0}) = \frac{|\mathbf{d}_{r,0}|}{|\mathbf{d}_r|} \exp \left\{ -j \frac{2\pi}{\lambda} (|\mathbf{d}_r| - |\mathbf{d}_{r,0}|) \right\}, \quad (2)$$

where λ is the carrier wavelength. Due to the separable form of $h(\mathbf{r}, \mathbf{s})$ between the transmitter and receiver, it is sufficient to study only the single-end Green's function. Therefore, the subsequent part of this paper will only study the Green's function at the receiver and omit the subscripts r and t used to denote the transmitter and receiver. To simplify the model, without loss of generality, we can always choose the origins of the transmitter and receiver coordinate systems to coincide with the reference antenna of the Tx/Rx array, and place the ULA symmetrically along the x -axis, where $\mathbf{r} = x\mathbf{e}_x$,

$x \in [-D/2, D/2]$ and \mathbf{e}_x is the unit vector of x -axis. Under such conditions, the expression for $|\mathbf{d}_r|$ in (2) is

$$|\mathbf{d}_r| = \sqrt{d_0^2 + x^2 - 2d_0x \cos(\phi)}, \quad (3)$$

where ϕ are the azimuth angle of the scatterer.

B. Wave-Number Domain Expression

Recently a novel channel model reflecting the angular characterization has been presented [12], which is called the Fourier plane-wave series expansion. By performing a Fourier plane wave transform on spatial channel response, it is decomposed into a series of weighted sums of plane waves in different directions, and the transformed domain is called the wave-number domain. The wave-number domain expression of the single-end spatial channel response function is

$$H(k_x, k_y) = \iiint_{-\infty}^{+\infty} dx dy dz h(\mathbf{r}) \cdot e^{-j(k_x x + k_y y + \sqrt{(2\pi/\lambda)^2 - k_x^2 - k_y^2} z)}. \quad (4)$$

Since we place the ULA symmetrically on the x -axis, then $y = z = 0$ and the range of integration in the spatial domain is changed to $x \in [-D/2, D/2]$. At this point, the expression of $H(k_x, k_y)$ is independent of k_y . Since the propagation of evanescent waves is not considered [12], the integral range of k_x is limited to $[-2\pi/\lambda, 2\pi/\lambda]$. Therefore, the wave-number domain expression of (4) can be reduced to the one-dimensional band-limited spectrum as

$$H(k_x) = \int_{-D/2}^{D/2} h(x) e^{-jk_x x} dx. \quad (5)$$

For the far-field path. When the azimuth angle of the far-field plane wave is ϕ , the expressions of $h(x)$ and $H(k_x)$ obtained from (5) are shown as

$$h_{far}(x) = \exp \left\{ j \frac{2\pi}{\lambda} \cos(\phi) x \right\}, \quad (6)$$

$$H_{far}(k_x) = \frac{2 \sin \left[\frac{D}{2} \left(k_x - \frac{2\pi}{\lambda} \cos(\phi) \right) \right]}{k_x - \frac{2\pi}{\lambda} \cos(\phi)}.$$

It can be observed that the power in the wave-number domain is mainly concentrated around $k_x = (2\pi/\lambda) \cos(\phi)$, thus the wave-number domain reflects the angular characteristics of multipaths.

III. WAVE-NUMBER DOMAIN APPROXIMATE EXPRESSION

A. Closed-form Approximation Based on POSP

By substituting the near-field single-end channel response (2) into the Fourier transform in the wave-number domain (5), the precise expression for the near-field angular domain channel can be obtained as

$$H_{near}(k_x) = \int_{-D/2}^{D/2} dx \frac{d_0}{\sqrt{d_0^2 + x^2 - 2d_0x \cos(\phi)}} \cdot \exp \left\{ j \left[-k_x x + \frac{2\pi}{\lambda} \left(d_0 - \sqrt{d_0^2 + x^2 - 2d_0x \cos(\phi)} \right) \right] \right\}. \quad (7)$$

The integrals shaped like (7) are known as oscillatory integral. It's difficult to obtain closed-form solution to (7) because of the presence of non-linear terms of x in phase of

the exponential part in (7), and the non-closed-form expression will make quantitative analysis challenging. But it is worth noting that oscillatory integrals are prevalent in FM signal processing, and a method called POSP [15] is widely used to approximate oscillatory integrals, which inspires us to take a similar approach to approximate (7).

Theorem 1 (the Principle of Stationary Phase [15]). *For an oscillatory integral of the form*

$$I = \int_{\Omega} A(x) \exp \{j\psi(x)\} dx, \quad (8)$$

where $A(x) > 0$ and the first-order derivative function of $\psi(x)$ is continuous. When $A(x)$ changing slowly and $\psi(x)$ changing rapidly with x , the integrand tend to oscillate rapidly, the positive and negative values tend to cancel each other. Only the integrand near the stationary point x_s , i.e., the first-order derivative $\dot{\psi}(x_s) = 0$, have contribution to I . Therefore, the approximation of I can be written as

$$I_{\alpha} = \sqrt{\frac{2\pi}{|\ddot{\psi}(x_s)|}} A(x_s) \exp \left\{ j \left[\psi(x_s) + \text{sgn}[\ddot{\psi}(x_s)] \frac{\pi}{4} \right] \right\}, \quad (9)$$

where $\ddot{\psi}(x)$ is the second-order derivative function of $\psi(x)$.

By comparing (7) and (8), the expressions of the magnitude and phase functions can be obtained as

$$A(x) = \frac{d_0}{\sqrt{d_0^2 + x^2 - 2d_0x \cos(\phi)}},$$

$$\psi(x) = -k_x x + \frac{2\pi}{\lambda} \left[d_0 - \sqrt{d_0^2 + x^2 - 2d_0x \cos(\phi)} \right], \quad (10)$$

where $\psi(x)$ have unique stationary point

$$x_s = d_0 \left[\cos(\phi) - \frac{k_x}{\sqrt{\left(\frac{2\pi}{\lambda}\right)^2 - k_x^2}} \sin(\phi) \right]. \quad (11)$$

Notice that the integral range of (7) is $\Omega_x = [-D/2, D/2]$, when $x_s \in \Omega_x$, k_x needs to be satisfied by

$$k_x \in \Omega_k = \left[\frac{\frac{2\pi}{\lambda} \left[\cos(\phi) - \frac{D}{2d_0} \right]}{\sqrt{1 + \left(\frac{D}{2d_0}\right)^2 - \frac{D}{d_0} \cos(\phi)}}, \frac{\frac{2\pi}{\lambda} \left[\cos(\phi) + \frac{D}{2d_0} \right]}{\sqrt{1 + \left(\frac{D}{2d_0}\right)^2 + \frac{D}{d_0} \cos(\phi)}} \right]. \quad (12)$$

Therefore, when $k_x \in \Omega_k$, the approximation of (7) can be obtained according to (9). When $k_x \notin \Omega_k$, the phase function $\psi(x)$ has no stationary points in the whole integral range Ω_x , then the integral is approximated to be 0. Thus we can obtain the closed-form approximation of (7) as (13).

The closed-form approximation (13) reflects the basic form of the near-field angular-domain channel: comparing to the far-field channel, where the power is all concentrated within a given width around $\frac{2\pi}{\lambda} \cos(\phi)$, the near-field model causes the power to diffuse, with the width of the diffusion becoming progressively wider as the distance d decreases. From (12), the diffusion region is not symmetric about $\frac{2\pi}{\lambda} \cos(\phi)$, it is always wider on the side where $|k_x|$ is smaller. In addition, the amplitude function of the near-field angular domain channel is a segment of a concave function, with smaller amplitudes at smaller $|k_x|$.

B. Simplified Expression

In the previous subsection, we obtained a closed-form approximation based on the POSP, which ignores the oscillatory effects of the angular domain channel and reflects its underlying trend. However, this expression is still complex. Fortunately, in practical near-field communication environments, the scatterer distances are generally not small enough to be of the order of the array aperture, hence $d_0 \gg D$. With this assumption, we can further simplify (13).

Specifically, by taking the Taylor series expansion as $D/d_0 \ll 1$, and retaining the first-order term, Ω_k can be approximate as

$$\Omega_k \approx \Omega_{k,s} = \left[\frac{2\pi}{\lambda} \left(\cos(\phi) - \frac{D \sin^2(\phi)}{2d_0} \right), \frac{2\pi}{\lambda} \left(\cos(\phi) + \frac{D \sin^2(\phi)}{2d_0} \right) \right]. \quad (14)$$

The $\Omega_{k,s}$ is symmetric about $\frac{2\pi}{\lambda} \cos(\phi)$, with a width of $\Delta(k_x) = \frac{2\pi D \sin^2(\phi)}{\lambda d_0}$. Since it has been assumed $D/d_0 \ll 1$, so when $k_x \in \Omega_{k,s}$, $|\frac{\lambda}{2\pi} k_x - \cos(\phi)| \ll 1$. Therefore, a Taylor series expansion of the amplitude of (13) around $k_x = \frac{2\pi}{\lambda} \cos(\phi)$ is performed, retaining only the first-order term, to obtain the simplified expression as (15).

The simplified expression (15) has a trapezoidal amplitude in angular domain. The center angle of the trapezoid is the far-field angle and the width is inversely proportional to the distance and related to the angle.

By the way, considering the angular resolution of an antenna array with an aperture of D is $\Delta_{array}(\cos(\phi)) = \frac{\lambda}{D}$, when the angular width $\Delta(k_x)$ is smaller than the angular resolution, the near-field effect cannot be observed by the antenna array

$$H_{close}(k_x) = \begin{cases} 0 & , k_x \notin \Omega_k \\ \sqrt{\frac{\lambda d_0}{\sqrt{1 - \left(\frac{\lambda k_x}{2\pi}\right)^2} \sin(\phi)}} \exp \left\{ j \left[d_0 \left(\frac{2\pi}{\lambda} - k_x \cos(\phi) - \sqrt{\left(\frac{2\pi}{\lambda}\right)^2 - k_x^2} \sin(\phi) \right) - \frac{\pi}{4} \right] \right\} & , k_x \in \Omega_k \end{cases} \quad (13)$$

$$H_{simp}(k_x) = \begin{cases} 0 & , k_x \notin \Omega_{k,s} \\ \sqrt{\frac{\lambda d_0}{\sin^2(\phi)}} \left\{ 1 + \frac{\cos(\phi)}{2 \sin^2(\phi)} \left[\frac{\lambda}{2\pi} k_x - \cos(\phi) \right] \right\} \exp \left\{ j \left[d_0 \left(\frac{2\pi}{\lambda} - k_x \cos(\phi) - \sqrt{\left(\frac{2\pi}{\lambda}\right)^2 - k_x^2} \sin(\phi) \right) - \frac{\pi}{4} \right] \right\} & , k_x \in \Omega_{k,s} \end{cases} \quad (15)$$

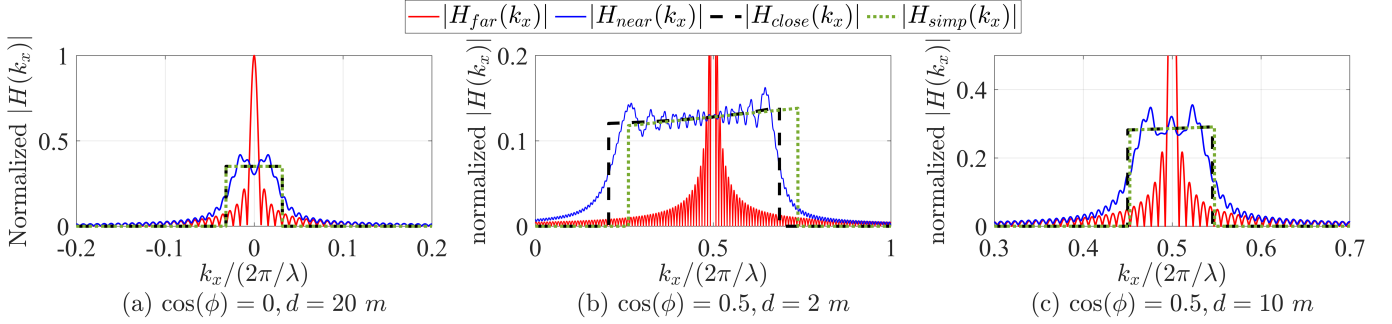


Fig. 2: The simulation of the normalized amplitude of angular domain channel.

system. Therefore, we have

$$\begin{aligned} \Delta(k_x) &< \frac{2\pi}{\lambda} \Delta_{near}(\cos(\phi)), \\ d_0 &> \frac{D^2 \sin^2(\phi)}{\lambda}. \end{aligned} \quad (16)$$

The expression in (16) can be defined as the near-field boundary based on the wave-number domain. Comparing (16) with the expression for Rayleigh distance, we can observe that they have a similar basic form. When $\phi = 0$, $\cos(\phi) = 1$, (16) equals half of the Rayleigh distance. Furthermore, (16) includes an additional $\sin^2(\phi)$ factor, indicating that the near-field region is not equidistant in all directions. This phenomenon has also been mentioned in ref. [17], where the Rayleigh distance shaped like (16) is also called effective Rayleigh distance.

IV. SIMULATIONS AND RESULTS

In this section, the accuracy and applicability conditions of the proposed two approximate expressions are verified through simulation. Firstly, numerical simulations of the wave-number domain channel are conducted. Examples with different parameters are provided to visualize the accuracy and differences of each model. Additionally, the PAS similarity percentage (PSP) is utilized to characterize the similarity of the wave-number domain channels, serving as a means to evaluate the approximation accuracy of the proposed model. In the simulation, without further elaboration, the ULA has $N = 256$ antennas and the spacing between antennas is $\lambda/2$. The carrier frequency is 30 GHz, so the Rayleigh distance of the ULA is 327.68 m.

A. Wave-Number Domain Numerical Results

First, the far-field wave-number domain channel $H_{far}(k_x)$ (6), the near-field wave-number domain channel $H_{near}(k_x)$ (7), and the two proposed approximation expressions $H_{close}(k_x)$ (13), $H_{simp}(k_x)$ (15) are simulated at different distances and angles, as shown in Fig. 2.

In Fig. 2. (a), the azimuth angle is 90° , and the distance is 20 m. At this point, the far-field channel $H_{far}(k_x)$ takes the form of a sinc function, while the near-field channel $H_{near}(k_x)$ exhibits a spread of power in the wave-number domain. Both approximation models can approximate the basic form of $H_{near}(k_x)$ while neglecting its oscillatory effects.

In Fig. 2. (b), the azimuth angle is 60° and the distance is 2 m, corresponding to an extreme near-field case. At this point, $H_{near}(k_x)$ is not symmetric with respect to $\cos(\phi) = 0.5$. The $H_{close}(k_x)$ model approximates this property more accurately, whereas $H_{simp}(k_x)$ produces a trapezoidal power distribution over a symmetric interval, which deviates from the exact value. This indicates that when the scatterers are extremely close to array, the $H_{close}(k_x)$ model provides a better approximation, while the $H_{simp}(k_x)$ model results in a larger error.

In Fig. 2. (c), the distance is increased to 10 m from Fig. 2. (b). At this point, there is almost no difference between $H_{close}(k_x)$ and $H_{simp}(k_x)$. Notably, the 10-meter distance is only 3% of the Rayleigh distance. This suggests that in most near-field environments, high accuracy can be achieved by using $H_{simp}(k_x)$ for approximation.

B. Similarity of Power Angular Spectrum

Furthermore, the accuracy and applicability of the proposed models are analyzed using a more quantitative approach. For wave-number domain channel response functions, one way to characterize their similarity is called PSP [16]. This approach first calculates $|H(k_x)|^2$ to obtain the normalized PAS, followed by the correlation coefficient between the two PAS distributions. The PSP between $|H_u(k_x)|^2$ and $|H_v(k_x)|^2$ can be expressed as

$$S_{u-v} = 1 - \frac{1}{2} \int \left| \frac{|H_u(k_x)|^2}{\int |H_u(k_x)|^2 dk_x} - \frac{|H_v(k_x)|^2}{\int |H_v(k_x)|^2 dk_x} \right| dk_x. \quad (17)$$

The similarity between $|H_{far}(k_x)|^2$ and $|H_{near}(k_x)|^2$ is denoted as S_{f-n} , the similarity between $|H_{close}(k_x)|^2$ and $|H_{near}(k_x)|^2$ is denoted as S_{c-n} , and the similarity between $|H_{simp}(k_x)|^2$ and $|H_{near}(k_x)|^2$ is denoted as S_{s-n} . The value of S_{c-n} and S_{s-n} can be used to illustrate the accuracy of the proposed model. The closer S_{c-n} and S_{s-n} is to 1, the more accurate the model is. Furthermore, the superiority of the proposed model over the plane-wave model can be illustrated by comparing S_{c-n} and S_{s-n} with S_{f-n} . In simulation, the distance varies from 1 m to Rayleigh distance while the angle varies from 0° to 180° . Results are shown in Fig. 3.

In Fig. 3, For the far-field channel model, the PSP is still 96.12% at the effective Rayleigh distance but decreases rapidly with decreasing distance, reaching 19.7% at 10 m. The proposed closed-form approximation has low accuracy under far-

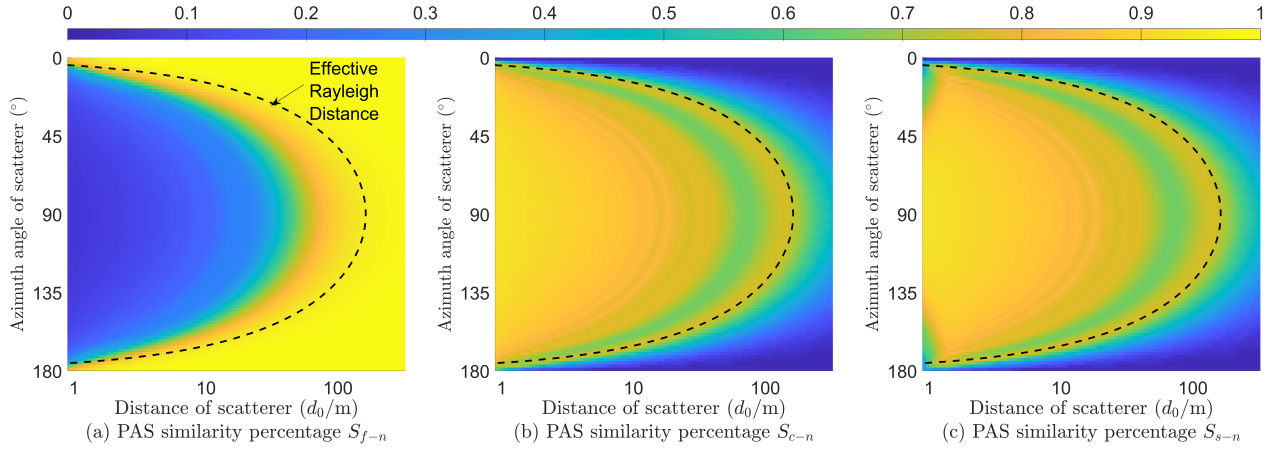


Fig. 3: The simulation of PSP S_{f-n} , S_{c-n} , S_{s-n} , with different d and ϕ . The black dashed line marks the near-field region determined by the effective Rayleigh distance, which is given by (16).

field conditions. However, within the effective Rayleigh distance, it achieves a minimum PSP of 64.89% and a maximum of 93.64%, precisely approximating the near-field channel. The proposed simplified approximation performs similarly to the closed-form approximation for $d > 2$ m. The accuracy decreases only when $d < 2$ m, with a minimum PSP of 38.28%.

In summary, the proposed closed-form approximation precisely approximates the near-field channel within the effective Rayleigh distance. Meanwhile, the simplified approximation achieves similar accuracy to the closed-form approximation when distance is larger than the antenna aperture.

V. CONCLUSION

In this paper, we discussed the expression of near-field wave-number domain channel and its approximation methods. We first presented a closed-form approximation based on POSP, which ignores the oscillatory effects of the wave-number domain channel and reflects its underlying trend. Then we proposed a simplified approximation under the condition that the scatterer distance is larger than the array aperture: a trapezoidal functions with linear phase. Finally, we verified the accuracy and applicability conditions of the proposed two expressions by simulation. Simulation results indicate that the proposed closed-form approximation can precisely approximate the near-field channel within the effective Rayleigh distance. Meanwhile, the simplified approximation can achieve similar performance to the closed-form approximation when the distance of scatterer is larger than the antenna aperture.

REFERENCES

- [1] J. Zhang, J. Lin, P. Tang *et al.*, “Deterministic Ray Tracing: A Promising Approach to THz Channel Modeling in 6G Deployment Scenarios,” *IEEE Commun. Mag.*, vol. 62, no. 2, pp. 48–54, Feb. 2024.
- [2] W. Saad, M. Bennis, and M. Chen, “A Vision of 6G Wireless Systems: Applications, Trends, Technologies, and Open Research Problems,” *IEEE Netw.*, vol. 34, no. 3, pp. 134–142, Oct. 2020.
- [3] J. Zhang, J. Lin, P. Tang *et al.*, “Channel Measurement, Modeling, and Simulation for 6G: A Survey and Tutorial,” *arXiv preprint arXiv:2305.16616*, 2023.
- [4] H. Miao, J. Zhang, P. Tang *et al.*, “Sub-6 GHz to mmWave for 5G-Advanced and Beyond: Channel Measurements, Characteristics and Impact on System Performance,” *IEEE J. Sel. Areas Commun.*, vol. 41, no. 6, pp. 1945–1960, May 2023.
- [5] K. T. Selvan and R. Janaswamy, “Fraunhofer and Fresnel Distances: Unified Derivation for Aperture Antennas,” *IEEE Antennas Propag. Mag.*, vol. 59, no. 4, pp. 12–15, Aug. 2017.
- [6] Y. Liu, Z. Wang, J. Xu *et al.*, “Near-Field Communications: A Tutorial Review,” *IEEE OpenJ. Commun. Soc.*, vol. 4, pp. 1999–2049, Aug. 2023.
- [7] X. Wei and L. Dai, “Channel Estimation for Extremely Large-scale Massive MIMO: Far-field, Near-field, or Hybrid-field?” *IEEE Commun. Lett.*, vol. 26, no. 1, pp. 177–181, Jan. 2022.
- [8] A. Yaghjian, “An Overview of Near-Field Antenna Measurements,” *IEEE Trans. Antennas and Propag.*, vol. 34, no. 1, pp. 30–45, Jan. 1986.
- [9] Z. Yuan, J. Zhang, Y. Ji *et al.*, “Spatial Non-Stationary Near-field Channel Modeling and Validation for Massive MIMO Systems,” *IEEE Transactions on Antennas and Propagation*, vol. 71, no. 1, pp. 921–933, Nov. 2023.
- [10] A. Paulraj and C. Papadias, “Space-Time Processing for Wireless Communications,” *IEEE Signal Processing Mag.*, vol. 14, no. 6, pp. 49–83, Nov. 1997.
- [11] A. Sayeed, “Deconstructing Multiantenna Fading Channels,” *IEEE Trans. Signal Process.*, vol. 50, no. 10, pp. 2563–2579, Oct. 2002.
- [12] A. Pizzo, L. Sanguinetti, and T. L. Marzetta, “Fourier Plane-Wave Series Expansion for Holographic MIMO Communications,” *IEEE Trans. Wireless Commun.*, vol. 21, no. 9, pp. 6890–6905, Sep. 2022.
- [13] Y. Zhang, X. Wu, and C. You, “Fast Near-Field Beam Training for Extremely Large-Scale Array,” *IEEE Wireless Commun. Lett.*, vol. 11, no. 12, pp. 2625–2629, Oct. 2022.
- [14] A. Pizzo, L. Sanguinetti, and T. L. Marzetta, “Spatial Characterization of Electromagnetic Random Channels,” *IEEE Open J. Commun. Soc.*, vol. 3, pp. 847–866, Apr. 2022.
- [15] E. Chassande-Mottin and P. Flandrin, “On the Stationary Phase Approximation of Chirp Spectra,” in *IEEE-SP Int. Symp. Time-Frequency Time-Scale Anal.*, 1998, pp. 117–120.
- [16] P. Kyösti, L. Hentilä, W. Fan *et al.*, “On Radiated Performance Evaluation of Massive MIMO Devices in Multiprobe Anechoic Chamber OTA Setups,” *IEEE Trans. Antennas Propag.*, vol. 66, no. 10, pp. 5485–5497, Oct. 2018.
- [17] M. Cui and L. Dai, “Near-field wideband beamforming for extremely large antenna arrays,” *arXiv preprint arXiv:2109.10054*, 2023.